Chemical Engineering Science 196 (2019) 54–63

Contents lists available at ScienceDirect

Chemical Engineering Science

journal homepage: www.elsevier.com/locate/ces

# Extracellular redox potential regulation improves yeast tolerance to furfural

Kai Li [a], Juan Xia [a], Muhammad Aamer Mehmood [a,b], Xin-Qing Zhao [a], Chen-Guang Liu [a,*], Feng-Wu Bai [a]

[a] State Key Laboratory of Microbial Metabolism, Joint International Research Laboratory of Metabolic & Developmental Sciences of Ministry of Education, School of Life Science and Biotechnology, Shanghai Jiao Tong University, Shanghai 200240, China
[b] Department of Bioinformatics and Biotechnology, Government College University Faisalabad, Faisalabad 38000, Pakistan

## HIGHLIGHTS

- Controlling extracellular redox potential enhances the tolerance of yeast to furfural.
- Intracellular redox status shows a tight correlation with extracellular redox potential.
- −100 mV is an optimal redox level to obtain high biomass and ethanol titer.

## GRAPHICAL ABSTRACT

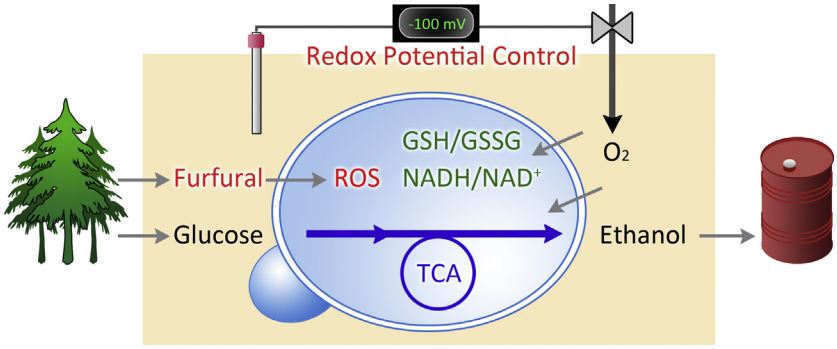


## ARTICLE INFO

*Article history:*
Received 7 August 2018
Received in revised form 3 November 2018
Accepted 30 November 2018
Available online 7 December 2018

*Keywords:*
*Saccharomyces cerevisiae*
Furfural
Stress tolerance
Redox potential
Ethanol fermentation

## ABSTRACT

Furfural is a major toxic byproduct present in the hydrolysate of lignocellulosic biomass, which inhibits the growth and ethanol fermentation of *Saccharomyces cerevisiae*. To enhance yeast tolerance to furfural, extracellular redox potential (ORP) regulation was employed for the fermentation system through controlling ORP at −150 mV, −100 mV and −50 mV, respectively, by adjusting its aeration. When ORP was controlled at −100 mV, yeast cells exhibited improved growth, furfural degradation and ethanol production. Analysis of intracellular redox pairs such as NADH/NAD$^+$ and GSH/GSSG indicated a correlation between extracellular ORP and intracellular redox homeostasis. Moreover, intracellular reactive oxygen species (ROS) caused by furfural stress decreased under the redox control condition, which consequently conferred yeast cells tolerance to furfural. Comparative transcriptome analysis for yeast cells sampling under the ORP control at −100 mV further revealed that the expression of genes for proliferation was up-regulated to degrade furfural more efficiently. These results demonstrated that extracellular ORP regulation would be a strategy for enhancing yeast tolerance to furfural stress during cellulosic ethanol fermentation.



## 1. Introduction

Fuel ethanol from lignocellulosic biomass such as forest wastes and crop residues has been believed to be an auspicious substitute of fossil fuels due to its social, environmental and economic sustainability (Ming and Dale, 2009). The main process of cellulosic ethanol production includes feedstock pretreatment, enzymatic hydrolysis of cellulose and ethanol fermentation (Chen et al., 2017). Pretreatment is a primarily step to address the recalcitrance of lignocellulose composed of cellulose, hemicelluloses and lignin which are intertwined together (Lynd et al., 2017). Unfortunately,

* Corresponding author.
*E-mail address:* cg.liu@sjtu.edu.cn (C.-G. Liu).

https://doi.org/10.1016/j.ces.2018.11.059
0009-2509/

toxic by-products are generated during the process, and compromise the growth and viability of yeast cells during ethanol fermentation. Furan derivatives, phenolic compounds and weak acids are common inhibitors, which are released during the pretreatment from cellulose, lignin, and hemicelluloses.

As a main degradation by-product of hemicelluloses in lignocellulosic biomass, furfural usually reaches to more than 4 g/L in corn cob hydrolysate after dilute acid pretreatment (Liu et al., 2004; Wang et al., 2011). Furfural inhibits the key enzymes of yeast involved in glycolysis and ethanol production (Jung et al., 2017; Taherzadeh et al., 2000). Moreover, furfural substantially disturbs the intracellular redox homogeneity through comprising the synthesis of intracellular reducing power NAD(P)H or accelerating its degradation. As a core cofactor, NAD(P)H participates in multiple essential processes of mass and energy metabolism (Liu et al., 2013). Strategies for rebuilding redox balance have been proven to assist yeast cells to overcome furfural inhibition (Wang et al., 2017; Jayakody et al., 2014).

Redox (oxidoreduction) potential (ORP) reflects valuable metabolic information with the cultivation of aerobic and anaerobic microorganisms (Schrader and Dehmlow, 2000). ORP of fermentation systems is a combination indicator for pH, dissolved oxygen and metabolism with a large number of redox pairs (Sato et al., 1998), and the intracellular redox balance and physiology of cells at multiple metabolic levels can be partially determined by extracellular ORP (Graef et al., 1999). Regulation of extracellular ORP has been shown to enhance stress tolerance of yeast to high-concentration ethanol (Liu et al., 2013). At the same time, chip analysis for gene expression also showed that the changes of ORP correlated with the expression of many stress response pathways such as the HSP family (Liu et al., 2013).

Since many inhibitors with aldehyde group such as furfural and vanillin cause imbalance of intracellular ORP (Wang et al., 2017), controlling ORP could be a primal choice to enhance the tolerance for yeast cells. Compared with genetic engineering that modifies metabolic pathway directly, process engineering aims to provide a proper environment for optimal cell metabolism without undertaking complicated strain modifications. There are three approaches often employed to control ORP including aeration tuning, reductant (oxidant) supplementation and electronic reactions (Liu et al., 2013), where accurate control on aeration is the most convenient method for aerobic or micro-aerobic fermentation, because oxygen with high standard redox potential is effective for altering ORP levels.

This study focused on the improvement of yeast tolerance to furfural during ethanol fermentation by adopting ORP control. The effect of extracellular redox levels on intracellular redox balance and metabolism were analyzed to depict mechanism underlying the enhancement of stress tolerance with yeast cells.

## 2. Material and methods

### 2.1. Media, yeast strain, and fermentation

The yeast strain BY4741 was cultured in the YPD medium composed of yeast extract (10 g/L), peptone (20 g/L), and glucose (20 g/L), to the mid-log phase (around 18 h) in shake flasks and inoculated into fermenter with 1 L working volume. The media in fermenter contained yeast extract (3 g/L), peptone (4 g/L), glucose (100 g/L), and furfural (4 g/L). A 10% inoculum was provided, and culturing was performed at 30 °C, pH = 4.5, at shaking speed of 150 r/min.

### 2.2. Redox control strategy

An autoclavable ORP electrode (model: Pt4805-DPAS-SC-K8S/225, Mettler Toledo, Switzerland) was implanted into the fermenter to monitor redox potential, and a known voltage signal was managed by a pH/ORP controller designed by the authors. When the known ORP value was dropped than the set point, 1 vvm filter-sterilized (0.2 μm nylon membrane) air was splashed into the fermenter until the ORP returned above the set point. ORP was maintained at: −50 mV, −100 mV, and −150 mV based on previous research (Liu et al., 2016). The aeration time was measured by PID algorithm built in the pH/ORP controller. No-aeration means no additional air supply during whole fermentation. Half-aeration was under aeration before 12 h and without air supply afterward. The stirring speed is 150 r/min for all.

### 2.3. Analyses

A 2-mL of the sample was collected from the fermentation broth every 12 h. Cells were removed by centrifugation (10,000*g* for 5 min), and the supernatant was subjected to glucose, ethanol, and furfural quantification using HPLC (Model: Waters 1525) with an RI detector (Model: Waters 2414) at 50 °C. An ion-exclusion column (Model: Aminex HPX-87H 300 × 7.8 mm, Bio-Rad, USA) was employed to separate the metabolites. $H_2SO_4$ (10 mmol/L) served as mobile phase at a flow rate of 0.6 mL/min (Qiu and Jiang, 2017; Wallace-Salinas and Gorwa-Grauslund, 2013). Cell growth was monitored by measuring optical density at 600 nm.

### 2.4. Measuring the intracellular redox potential

Intracellular values of the GSSG/GSH redox potential ($Eh_{GSSG/2GSH}$) and NADH/NAD$^+$ redox potential ($Eh_{NADH/NAD}$) were calculated from concentrations of redox pairs using the Nernst equation (Drakulic et al., 2005):

$$Eh_{GSSG/GSH} = E_{0GSSG/GSH} + 2.303\frac{kT}{nF}\log_{10}\frac{[GSSG]}{[GSH]^2} \quad (1)$$

$$Eh_{NAD/NADH} = E_{0NAD/NADH} + 2.303\frac{kT}{nF}\log_{10}\frac{[NAD]}{[NADH]} \quad (2)$$

$E_{0GSSG/GSH}$ and $E_{0\ NAD/NADH}$ are the standard potentials for GSSG/GSH (−0.24 V) and NAD/NADH (−0.32 V) at pH 7. Where "k" is the Boltzmann's constant (8.31 J/mol/K), "T" is the absolute temperature, "n" is the number of electrons transferred, and "F" is the Faraday's constant (96406 J/V).

### 2.5. Measurements of intracellular GSH, NADH, and ROS

NADH and NAD$^+$ concentrations were measured using a kit in accordance with the manufacturer's instructions (Qiao Suo Co., Ltd., Shanghai, China). Briefly, the NADH cycling assay was performed using Spectra Fluor Plus in a 96-well plate format. The reaction mixture comprised 40 μL sample extract, 16 μL bicine (1.0 mol/L, pH = 8.0), 40 μL neutralizing buffer (0.1 mol/L NaOH for NAD$^+$ or 0.1 mol/L HCl for NADH), 16 μL phenazine ethosulfate (PES), 16 μL 3-[4,5-dimethylthiazol-2-yl]-2,5-diphenyltetrazolium bromide (MTT), 16 μL absolute ethanol (~100%), and 30 μL EDTA (40 mmol/L, pH = 8.0). At the end, the PES and MTT were added to the 96-well plate, and the mixture was incubated at 30 °C for 3 min. Next, 3.2 μL of alcohol dehydrogenase (500 U/mL) prepared in the bicine buffer (pH = 8.0) was added to the reaction mixture to initiate the reaction assay. An increase in absorbance (570 nm) was recorded within 10 min. The rate of reduction of MTT is proportional to the concentration of NAD$^+$ or NADH in the sample. Known concentrations of NAD$^+$ (0.0375 nmol/L) and NADH (0.75 nmol/L) were applied to calibrate the assay. A 2′,7′-dichlorodihydrofluorescein diacetate (DCFH-DA)-based kit (Beyotime Institute of Biotechnology, China) was used to quantitate reactive oxygen species (ROS). Yeast samples treated with gold nanoparticles (10 μg/mL)

for 4 h by centrifugation were stained with 10 μmol/L DCFH-DA. Fluorescence intensity of ROS was estimated by a microplate reader (Tecan Infinite 200) with excitation set at λ 488 nm and emission at 525 nm (Allen et al., 2010).

GSH and GSSG levels were measured using commercial kits (Beyotime Biotechnology, Nantong, China) following the manufacturer's protocol. Cells ($2 \times 10^5$/mL) were seeded into 6-well plates and treated with different benzoquinone concentrations (0, 10, and 20 μmol/L) for 24 h. The cells were washed with phosphate-buffered-saline, and protein removal agent was added. The samples were freeze-thawed twice with liquid nitrogen in a water bath at 37 °C. The cells were clarified by centrifugation (10,000*g*) for 10 min at 4 °C. The supernatant was used for the measurement of GSH and GSSG at 450 nm using a microplate reader. All chemicals used were of analytical grade and were purchased from Sigma or other vendors of equivalent standards (Wang et al., 2016).

### 2.6. Transcriptome analysis

Samples were collected 48 h after inoculation at the fermentation stage. Cell pellets were clarified by centrifugation (8000 *g*, 5 min, at 4 °C) and then were immediately frozen in liquid nitrogen. Total RNA was extracted by Spin Column Plant total RNA Purification Kit (Sangon, Shanghai, China) according to the manufacturer's instructions. RNA-Seq analyses were performed on two independently replicated fermentation experiments to ensure reproducibility of results. Agilent 2100 Bioanalyzer was used for determining RNA quality and quantity. Total RNA was submitted to NovelBio for processing and chip hybridization following the instructions of the manufacturer (Bio-Pharm Technology Co., Ltd). The arrays were scanned with the Agilent Microarray Scanner (Agilent p/n G2565BA), and the data were extracted using featured software (Agilent Feature Extraction software). Normalization was performed by the robust multi-array average (RMA) method (Zhang et al., 2016, 2013). Differentially expressed genes were determined through gene ontology (GO) and a web-based software GOEAST (Zheng and Wang, 2008). Fisher's exact test was employed to classify the GO categories, and the false discovery rate (FDR) was determined to correct the *P-value* (Prieto et al., 2008).

## 3. Results and discussion

### 3.1. Effect of inhibitors on yeast growth

Corn stover is an abundantly available feedstock for lignocellulosic ethanol production. Industrial scale pretreatment of lignocellulose often involves the use of a dilute acid due to the low associated costs and availability of established technology. We sought to determine the effect of inhibitors resulting from acid pretreatment on the growth of *Saccharomyces cerevisiae* in the presence of 4 g/L acetic acid, 1 g/L 5-HMF, or 4 g/L furfural (Fig. S1), similar concentrations of which are known to accumulate in the corn stover hydrolysate after acid pretreatment. While 1 g/L 5-HMF showed no significant inhibitory impact on cell growth, 4 g/L acetic acid and 4 g/L furfural were found to prolong the lag phase in yeast by 12 and 36 h, respectively. Furfural was therefore identified to be the major inhibitor of yeast growth in corn stover hydrolysate after acid pretreatment. 4 g/L furfural was consequently used in the following experiments to study the impact of ORP-mediated regulation of furfural tolerance.

### 3.2. Yeast growth and fermentation under redox potential control

All fermentation experiments exhibited almost similar redox profiles (Fig. 1A). Yeast cultured in freshly prepared media exhibited vigorous growth resulting in rapid depletion of dissolved oxygen in the broth; degradation of carbohydrates was associated with increase in reducing power and reduction of oxidizing power in the medium resulting in a radical decline in ORP from 70 to −220 mV. However, redox-control and half-aeration performed during the early 12 h of growth were found to increase the redox value. ORP control was initiated at 18, 28, and 46 h to be maintained at −50, −100, and −150 mV, respectively. The half-aeration group with no air supply after 12 h showed an ORP drop to −176 mV at the end of fermentation.

The yeast cells grown under no-aeration (the control) displayed a prolonged lag phase of 36 h due to the inhibitory effect of furfural (Fig. 1B). On the contrary, the other groups grown under aeration for the first 12 h exhibited much greater biomass and specific growth rate. Yeast maintained under an ORP of −50 mV displayed the greatest acceleration in growth during the first 24 h and through 48 h; because it reached the set value of −50 mV was attained within 18 h with the aeration supplied in the early stages of growth.

The glucose consumption in the cultures that received no aeration was found to be significantly reduced with 15 g/L residual glucose measured at 72 h (Fig. 1C). Aeration during the first 12 h of growth was found to alleviate this problem and increase glucose utilization; the aerated groups displayed elevated rates of glucose consumption and were able to reduce glucose levels to about 8 g/L by 72 h. Maintenance of ORP further promoted glucose utilisation, under which state the yeast exhausted the glucose by 72 h. Maintenance of cultures at −50 mV led to sugar depletion even faster by around 60 h.

The ethanol accumulation is shown in Fig. 1D. No-aeration group produced the least ethanol because of the lowest glucose consumption. The −50 mV group displayed the fastest rate of ethanol production before 60 h. The ethanol production, however, decreased by 72 h due to the depletion of glucose and aeration stripping loss. The optimal conditions for efficient fermentation by yeast were determined to be at an ORP of −100 mV.

Glycerol is a major by-product of ethanol fermentation by *S. cerevisiae* (Medina et al., 2010). As shown in Fig. 1E, the final concentration of glycerol produced by yeast in the redox-controlled group was much higher than in the no-aeration group. The highest concentration of glycerol attained in group maintained at −50 mV was 3 g/L, which was 0.4 g/L higher than what was seen in the no-aeration controls.

The consumption of furfural is illustrated in Fig. 1F. Yeast cells with no-aeration consumed the furfural by 48 h, whereas, cells in half-aeration group (that only received aeration for the initial 12 h) were able to consume furfural faster, by 36 h; ORP-controlled groups displayed moderately accelerated furfural consumption compared to that seen in the half-aeration group. Aeration during the initial stages of yeast growth was, therefore, found to play an important role in the detoxification of furfural.

Overall, aeration improved cell growth and utilization of furfural and glucose that was correlated with an increase in ethanol titres. Groups under ORP control displayed better and faster ethanol fermentation with high ethanol titres.

### 3.3. Aeration statement for redox potential control

As a result of the common aeration step, the redox-controlled groups and those subjected to only the initial aeration (the half-aeration group) showed similar profiles of growth and fermentation during the first 12 h (Fig. 1). The redox-controlled group eventually displayed better overall growth and fermentation compared to its non-redox controlled counterpart. As expected, the redox-controlled groups maintained at −50 mV showed the best growth owing to the greatest air volume; the biomass of groups

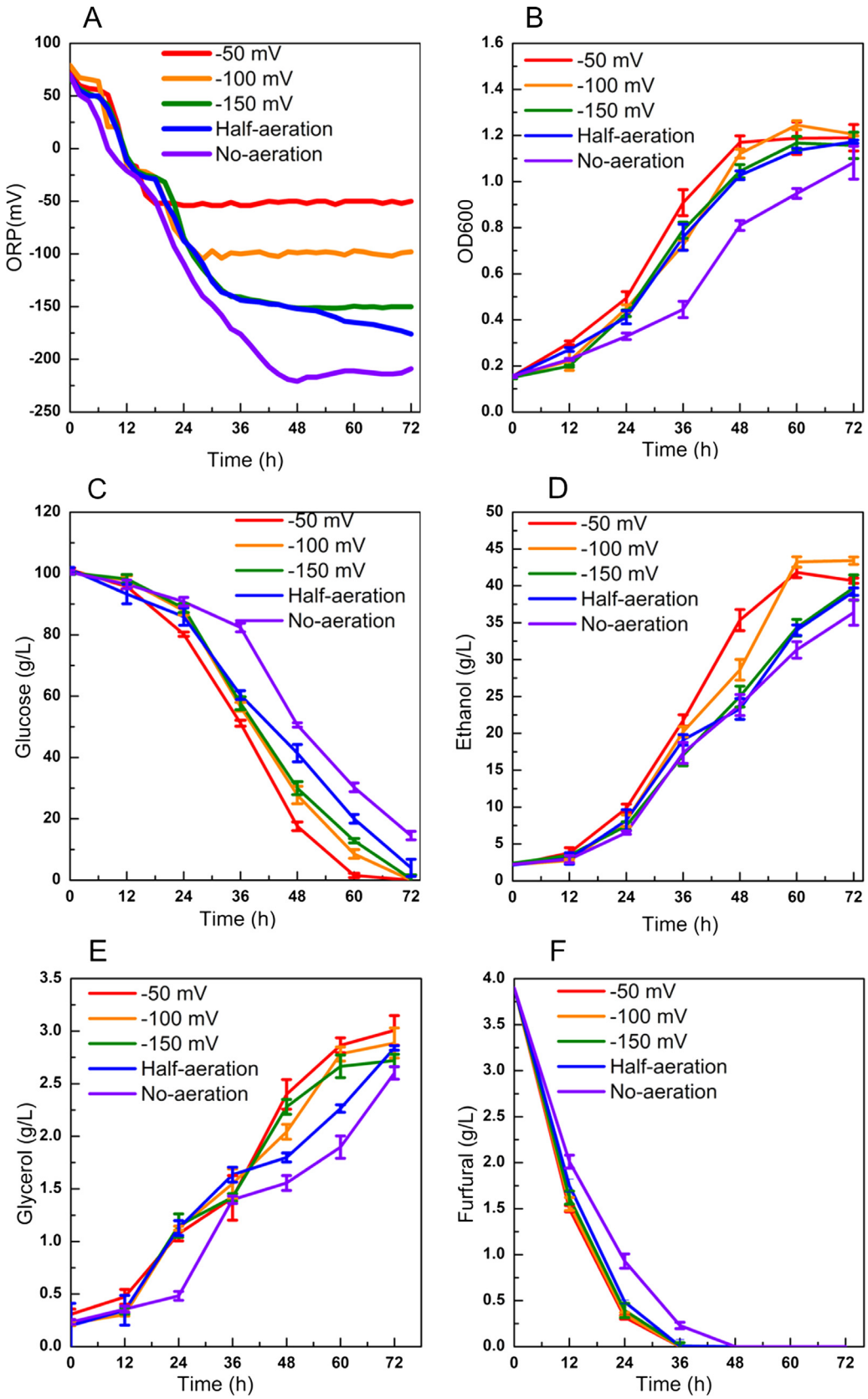


**Fig. 1.** Performance of ethanol fermentation under redox potential regulation in presence of 4 g/L furfural. (A) ORP profile; (B) Cell growth; (C) Glucose consumption; (D) Ethanol production; (E) Glycerol accumulation; (F) Furfural degradation. Error bars indicate standard deviation of biological triplicates.

maintained at an ORP of −100 or −150 mV were found to be a function of their aeration volume as well. The pathway of cellular respiration fuelled by oxygen is likely to generate enough energy to promote both cellular proliferation and furfural stress tolerance.

As shown in Fig. 2, during the first 12 h of growth, the half-aeration and redox-controlled groups were aerated with constant air flow at the rate of 0.07 vvm. In the half-aeration group, the aeration was stopped at 12 h. The −50 mV redox-controlled group was created via manipulated-aeration beginning at the 18 h incubation mark; similar aeration strategies were adopted beginning at the 28 and 46 h incubation point to maintain the redox potential of two other groups at −100 and −150 mV, respectively. The group maintained at −50 mV ORP received aeration for the longest period accounting for the greatest aeration volume; however, for the redox-controlled group maintained at −150 mV, only a little air was sparged into the fermenter during ORP manipulation. The aeration volume of groups maintained at −50 mV displayed a 49.82% increase over the aeration-induced volume of group maintained at −100 mV. Similarly, the aeration-induced volume was 4.71% higher in group maintained at −100 mV than in group maintained at −150 mV. Likewise, the aeration-induced volume was found to be 1.01% higher in group maintained at −150 mV than in the half-aeration group that did not receive redox maintenance. Overall, this indicates that the maintenance of higher ORP levels during ethanol fermentation requires much more air, which could lead to problems including contamination, ethanol loss, and high energy costs. Notably, despite the small difference between the aeration-induced volume of the −150 mV controlled and half-aeration groups (only 1.01%), yeast cells controlled at −150 mV consumed more glucose at the rate of 10 g/L when compared to half-aeration group (Fig. 1C). This is suggestive that a little aeration can bring about a significant tolerance to stress. It remains to be clarified if stress tolerance in yeast cells is a direct consequence of the amount of oxygen from the aeration or an indirect effect of ORP regulation by oxygen.

### 3.4. The main redox metabolites in yeast under redox potential control

Since significant differences in cell growth, glucose utilization, and ethanol production were observed between the no-aeration and redox-controlled conditions, it was essential to monitor the intracellular redox metabolites in response to extracellular ORP control, to elucidate the correlation between intra and extracellular redox potential. The highest ethanol titre was observed in the ORP-controlled group at −100 mV; this group was, therefore, compared with the no-aeration group for the presence of intracellular redox metabolites such as cofactors, ROS, and glutathione, in the presence of furfural.

Cofactors are involved in several metabolic reactions that specifically affect redox balance and cellular processes overall (Holm et al., 2010). As illustrated in Fig. 3A, the lowest ratio of $NADH/NAD^+$ was measured at 12–24 h, during the lag phase, when yeast cells re-adjust their metabolic profile for a new environment with low reducing power due to low glucose consumption. There was no significant difference in the $NADH/NAD^+$ ratio between the no-aeration and −100 mV redox-controlled groups at all except the 36 h point, which was indicative that the cells preferred to maintain the intercellular redox homogeneity even though the extracellular redox changed dramatically. The ratio of $NADH/NAD^+$ in the −100 mV group was found to be higher than in the no-aeration group at 36 h. While cells without aeration had just begun the exponential phase because of furfural inhibition, cells maintained at −100 mV were in the mid-exponential phase of growth vigorously metabolising carbohydrates with an accompanied increase in the reducing power. Another potential reason for the higher $NADH/NAD^+$ ratio in the cells maintained at −100 mV could be the detoxification of furfural which is an NADH requiring process. Consistent with this reasoning, yeast cells at −100 mV consumed furfural earlier when compared to the no-aeration group, which means more reducing power was conserved.

ROS is a common family of oxidants that damages cell components and is associated with universal stress responses including that induced by furfural (Allen et al., 2010). Thus, intracellular ROS content could be an indicator of the furfural stress, in addition to the oxidative stress induced by ORP control. Fig. 3B shows that ROS fluorescence intensities in the −100 mV ORP-controlled group at 12 h and 24 h were much higher than that in the no-aeration group; this is consistent with the yeast cells in the −100 mV ORP group being subjected to not only the furfural-induced stress but also the oxidative stress caused by aeration during the first 24 h. The synergetic effect of aeration and furfural is likely to account for the high ROS content. After 24 h, however, yeast cells under the −100 mV control were able to quickly consume furfural; the constant aeration was replaced by accurate ORP control with small, regulated bouts of aeration which led to alleviation of the stress and consequently reduced intracellular ROS. On the other hand,

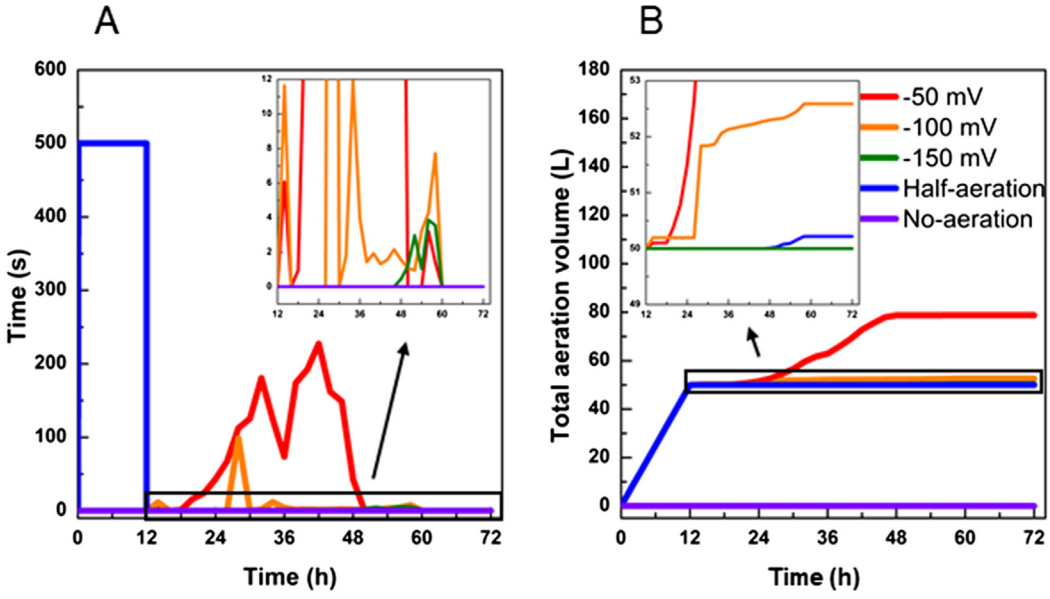


**Fig. 2.** Aeration time (A) and total air volume (B) pumped into fermenter during redox potential-controlled ethanol fermentation.

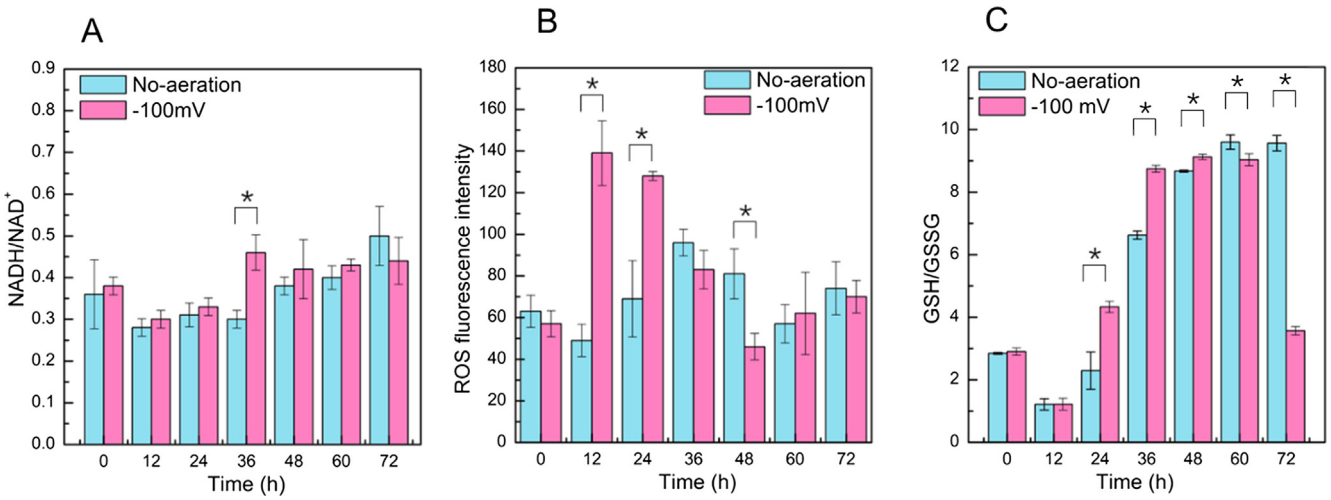


**Fig. 3.** Main redox metabolites in −100 mV redox potential control group and no-aeration group. (A) Ratio of NADH/NAD$^+$; (B) ROS; (C) Ratio of GSH/GSSG; *: significant difference *P-value* < 0.05. Error bars indicate standard deviation of biological triplicates.

yeast cells in the no-aeration group took longer to degrade the furfural leading to increase in production of ROS until 48 h. The ROS content of the cells in the no-aeration group was, therefore, higher when compared to that in cells in the −100 mV group between 36 and 48 h. After 48 h, neither aeration nor furfural caused the accumulation of ROS indicated by the reduction in fluorescence intensity of ROS comparable to that seen in cells at 0 h. No significant difference was observed between the −100 mV controlled and no-aeration groups by this point.

The glutathione (GSH) reduction system helps in the maintenance of a reduced environment in the *S. cerevisiae* cytosol (Rouhier et al., 2010). Reduced GSH can be regenerated from oxidized GSSG utilizing the reducing power of NADPH. Sufficient reducing power in the cytosol is, therefore, important for a high GSH/GSSG ratio. The breakdown of glucose serves as a pivotal source of reducing power in the cell; a correlation can, therefore, be established between residual glucose profiles and GSH/GSSG ratios. As shown in Fig. 3C, cells were found to have a low ratio of GSH/GSSG at 12 h in both the no-aeration and −100 mV-controlled groups as a result of slow glucose utilization due to furfural stress. Entry of the −100 mV controlled cells into the exponential phase at 24 h was accompanied by rapid glucose consumption resulting in a 2–3 fold increase in the GSH/GSSG ratio that was found to prevail until depletion of glucose at 60 h; a steep fall in the GSH/GSSG ratio was observed by 72 h. In contrast, cells in the no-aeration group were delayed in their entry into exponential phase displaying rapid consumption of glucose by 36 h and a subsequent increase in GSH/GSSG the ratio. These observations indicate that the control of ORP not only influenced the extracellular redox potential but also contributed to the intracellular metabolic and redox shift.

### 3.5. Correlation of extracellular and intracellular redox potential

The above results have revealed that regulation of extracellular redox potential improves the resistance to furfural. We were, therefore, interested to determine if there was a correlation between the redox status inside and out of the cell. Cells tend to maintain an intracellular redox balance; hence, the measured $Eh_{(NAD+/NADH)}$ and $Eh_{(GSSG/GSH)}$ were found to vary within very narrow ranges (50–110 mV) despite relatively wide variations in the environmental ORP varying from (−250 - 100 mV). In addition, the values of $Eh_{(NAD+/NADH)}$ and $Eh_{(GSSG/GSH)}$ between the two no-aeration and −100 mV redox controlled groups were not found to be significantly different (Fig. S2). The ability of yeast cells to attenuate the effect of extracellular ORP fluctuations can be attributed to the cytomembrane barrier and to metabolism regulation. As mentioned in Section 3.2, the ORP was found to decrease gradually and finally become stable at −100 mV and around −220 mV in the ORP controlled and no-aeration groups, respectively, the persistent reducing power being driven by the catabolism of carbohydrates.

Intracellular values of the GSSG/GSH half-cell redox potential ($Eh_{(GSSG/GSH)}$) were determined during whole phases as an indicator of the cellular redox environment (Schafer and Buettner, 2001). A similar trend was noted with $Eh_{(NAD+/NADH)}$ where a decrease in the first 12 h was followed by a gradual increase. These observations are indicative that extracellular redox can influence the intracellular redox balance, although the relationship is indirect.

The profiles of extracellular redox potential, $Eh_{(NAD+/NADH)}$, and $Eh_{(GSSG/GSH)}$ were found to consistently decrease between 0 and 12 h. At the start of fermentation, yeast cells in exponential phase with abundant reducing power were inoculated into fresh medium rich in dissolved oxygen and a high ORP. The huge differences between the extracellular and intracellular redox status stimulate the cells to adjust metabolism pathways to acclimatize into the fresh medium as is seen in the lag phase; the cellular redox status is, consequently, observed to climb to a higher ORP level within 12 h. It must be clarified that extracellular as well as intracellular redox potential is the sum of individual redox potentials of all substances comprising the redox environment. Each substance that can be oxidized or reduced has its own redox potential range. $Eh_{(GSSG/GSH)}$ is known to be in the range of −260 to −370 mV, whereas $Eh_{(NAD+/NADH)}$ is in the range of −220 to −270 mV. An accurate intracellular redox potential can, therefore, be calculated if the concentrations of all redox pairs in the cell are known. Current methods, unfortunately, use concentrations of a few representative redox metabolites revealing only metabolite-specific redox potential that gives only a partial glimpse of the intracellular ORP.

### 3.6. Differential gene expression between redox-controlled and no-aeration groups

The mRNA fractions purified from mid-exponential phase (48 h) cells cultured at −100 mV ORP and from the no-aeration group were subjected to gene expression profiling for the identification of differentially expressed genes. Taking $\log_2$(−100 mV/no-control) > 2 or <−2 as a criterion, it was shown that 52 genes were

up-regulated while 41 were down-regulated in the −100 mV controlled cells relative to the gene expression profile of the no aeration group of cells. These genes were subjected to GO enrichment analysis, and catalogues were then sorted in the descending order in accordance with $-\log_{10}(P\text{-}value)$ (Table S1).

Among the up-regulated genes, 10 enrichments (Fig. 4A) were shown to be related to the protein biosynthetic pathway, 7 groups were shown to be related to rRNA processing and ribosome biogenesis, and 3 groups were found to be involved in the mRNA polymerase-I promoter. Examples include *SPB1* (fold change 2.11), involved in rRNA processing and 60S ribosomal subunit maturation (Bonnerot et al., 2003); *BFR2* (fold change 2.31), an essential protein component of 90S pre-ribosomes that may be involved in rRNA processing (Soltanieh et al., 2014); and *SSF1* (fold change 2.17), that encodes integral proteins of 66S pre-ribosomal particles and is required for the maturation of the larger ribosomal subunit (Bogengruber et al., 2003). The convergent synthesis of mRNA, tRNA, and ribosomes in yeast cells under ORP control could account for the apparent growth advantage in these cells. The faster cell growth in the −100 mV ORP group, facilitated the rapid breakdown of furfural, depleting furfural from the medium within 48 h.

The down-regulated genes were shown to be related mainly to carbohydrate metabolism, glycogen biosynthesis, and the pentose phosphate shunt (Fig. 4B). Examples of these genes included *GSY1* (fold change −2.62) and *ZWF1* (fold change −1.37). *GSY1* is a glycogen synthesis gene that is induced by glucose limitation. Furfural-mediated reduction of the rate of glucose assimilation (despite high glucose levels in the medium during the early stages of growth) in the no-aeration group could have stimulated the cells to synthesize glycogen. *ZWF1*, on the other hand, is a glucose-6-phosphate dehydrogenase (G6PD) which catalyses the first step of the pentose phosphate pathway and may be involved in cellular adaptation to oxidative stress. There is lesser oxidative stress experienced by cells maintained at −100 mV than those subjected to no-aeration. Consequently, cells in −100 mV controlled state do not need to synthesize as much NADPH (compared to cells in the no aeration group) via pentose phosphate pathway to eliminate the oxidative stress caused by furfural.

The two main categories of stress response in cells include oxidation-reduction reactions and the trehalose biosynthetic process. The detoxification of furfural has been shown to be an oxidation-reduction reaction; furfural can be reduced to furfuryl alcohol using molecular NADH. Trehalose is known as a protective agent in cells and is present under various circumstances of stress. The genes down-regulated in the ORP controlled group were reflective of the stress status of the cell and this regulation was relieved after 48 h. Therefore, the yeast cells under −100 mV controlled ORP initially invested in the synthesis of proteins to detoxify furfural followed by the subsequent activation of carbohydrate metabolism pathways.

### 3.7. Glucose metabolism at the transcriptional level

To analyse glucose catabolism, the transcriptome was superimposed on the metabolic network to further analyse changes in cells maintained at −100 mV controlled ORP relative to cells in no-aeration groups (Fig. 5).

Genes involved in the glycerol synthesis pathway, including *GUT1* (glycerol kinase), *GPD1*, and *GPD2* (glycerol-3-phosphate dehydrogenase) (Albertyn et al., 1994) were down-regulated in the −100 mV controlled group because NADH generation was surpassed as shown in Fig. 3. The expression of *TDH2*, on the other hand, was upregulated; *TDH2* that encodes glyceraldehyde-3-phosphate dehydrogenase catalyses the conversion of glyceraldehyde-3-phosphate to 1,3 bis-phosphoglycerate was enhanced. There was a shift in carbon flux to the ethanol pathway but not to glycerol synthesis. Additionally, the *PDC1* gene encoding a pyruvate decarboxylase was up-regulated; this gene product increases the carbon flux to both acetic acid and ethanol. However, acetic acid concentration in the −100 mV controlled group was not significantly higher when compared to the no-aeration group due to the down-regulation of *ALD3* that encodes aldehyde dehydrogenase to convert acetaldehyde to acetic acid (Navarro-Aviño et al., 1999). Ethanol production was, hence concurrently increased. Taken together, ORP maintenance favours the ethanol synthesis pathway rather than the glycerol or acetic acid synthesis pathways in the presence of furfural. It implies that proper ORP level not only determines the metabolic reaction via changing the ratio of cofactors but also regulates the expression of genes that are involved in fermentation. In brief, ORP shifts metabolic flux, though the change was not significant because of the robust fermentation pathways in yeast that maintain the stability of metabolic flux.

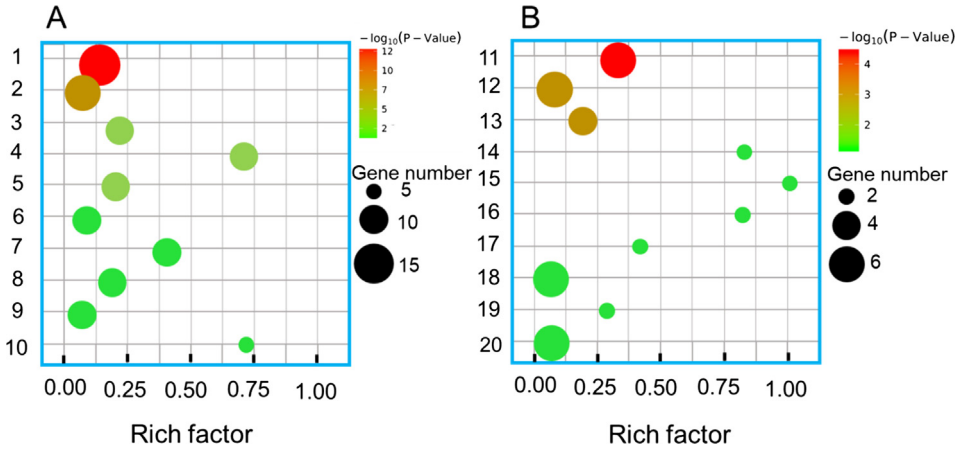


**Fig. 4.** Pathway enrichment of different expression genes between −100 mV and no-aeration. (A) Up-regulated genes; (B) Down-regulated genes. The numbers labeled in Y-axis stand for the enriched pathways and the sphere size represents the gene number 1: ribosome; 2: rRNA processing; 3: rRNA methylation; 4: positive regulation of transcription from RNA polymerase I promoter; 5: ribosomal large subunit biogenesis; 6: maturation of SSU-rRNA transcript; 7: maturation of LSU-rRNA tricistronic rRNA transcript; 8: ribosomal large subunit assembly; 9: transcription of nuclear large rRNA transcript from RNA polymerase I promoter; 10: regulation of transcription from RNA polymerase I promoter; 11: glycogen biosynthetic process; 12: carbohydrate metabolic process; 13: pentose-phosphate shunt; 14: polyamine catabolic process; 15: beta-alanine biosynthetic process; 16: glycogen catabolic process; 17: pentose-phosphate shunt, oxidative branch; 18: oxidation-reduction process; 19: trehalose biosynthetic process; 20: metabolic process.

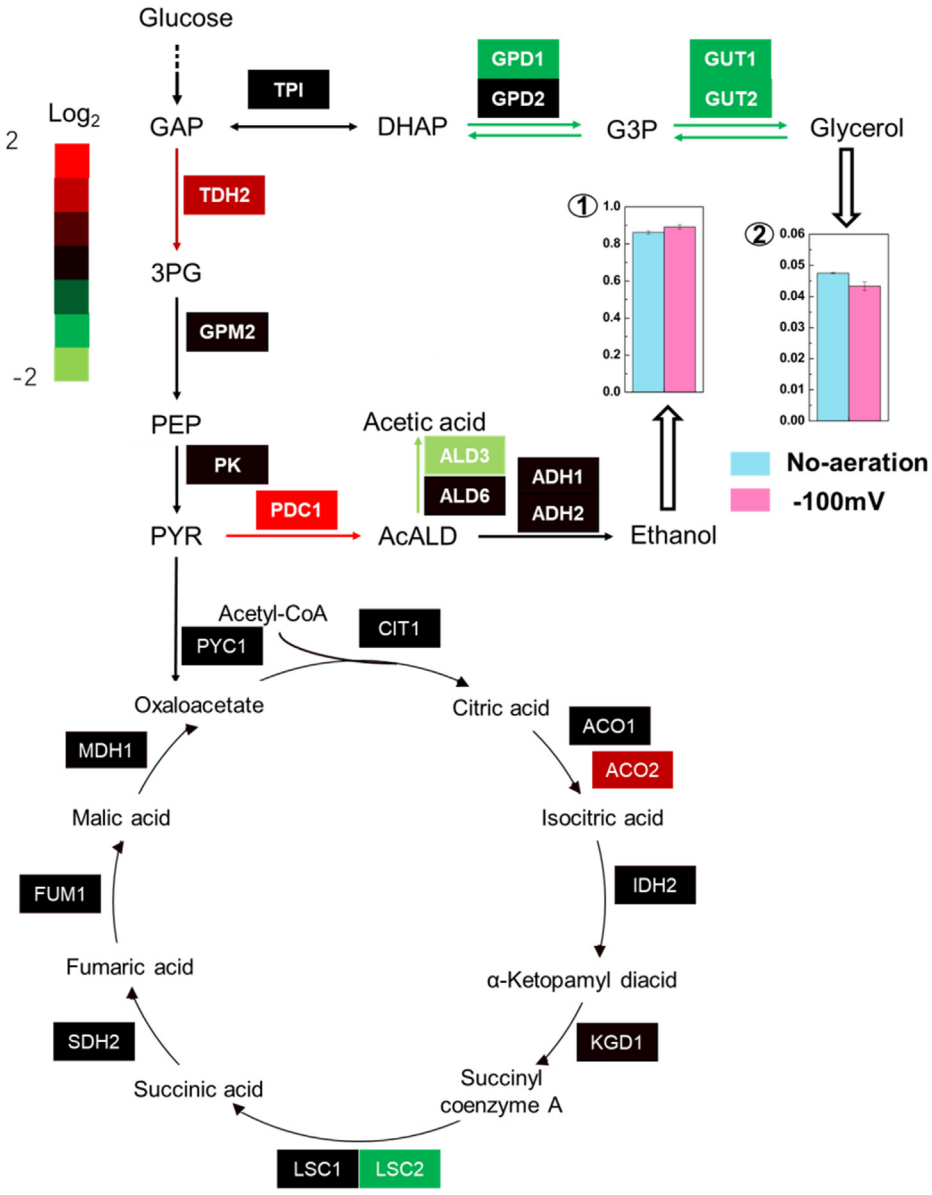


**Fig. 5.** Transcription response of yeast cells in the late-exponential phase superimposed on ethanol, glycerol and TCA metabolism. Expression of genes in −100 mV vs. no-aeration group is indicated in red for up-regulation and green for downregulation. GAP: glyceraldehyde-3-phosphate; DHAP: dihydroxyacetone phosphate; G3P: 3-phosphoglycerate; 3PG: 3-Phosphoglyceric acid; PEP: Phosphoenolpyruvic acid; PYR: Pyruvic acid; AcALD: acetaldehyde; GUT1/2: glycerol kinase; GPD1/2: glycerol-3-phosphate dehydrogenase; TDH2: glyceraldehyde-3-phosphate dehydrogenase; PK: phosphoenolpyruvate carboxykinase; PDC1: pyruvate decarboxylase; ALD3/6: aldehyde dehydrogenase; ADH1/3: alcohol dehydrogenase. ①: Specific ethanol production rate; ②: Specific glycerol production rate. Error bars in ① and ② indicate standard deviation of biological triplicates. (For interpretation of the references to colour in this figure legend, the reader is referred to the web version of this article.)

Interestingly, the TCA pathway did not exhibit changes under the ORP controlled compared to no aeration conditions despite 52 L of aeration volume in the −100 mV controlled group. ORP control is not just a simple aeration process but involves an accurate redox-based modulation of metabolism for efficient ethanol production and robust stress tolerance. In this case, the ORP controlled group seemed to increase ethanol production mainly through the enhancement of strain growth rather than upregulation of ethanol synthesis genes. Extracellular ORP control exhibited greater effects on cytoplasmic enzymes than on TCA-related enzymes in the mitochondria; this was indicative that extracellular ORP is tightly correlated with the cofactors in the cytoplasm but has less influence on the mitochondrial cofactors due to compartmental isolation.

### 3.8. Oxidative stress-responsive genes

Expression of selected genes involved in endogenous antioxidant defence was also studied under furfural stress during the exponential phase (48 h) in the −100 mV controlled group (Fig. 6). The expression levels of all genes were found to be decreased significantly compared to the no-aeration group (expect for *GSH1*). As mentioned above, furfural was depleted by 36 h in −100 mV ORP group but was present even after 48 h in the no-aeration group. Thus, the presence of furfural led to the upregulation of most genes as part of the antioxidant response. The function of some of these genes are as follows: *CTA1* and *CTT1* encode peroxisomal catalases (catalase A and T) in the cytosolic matrix,

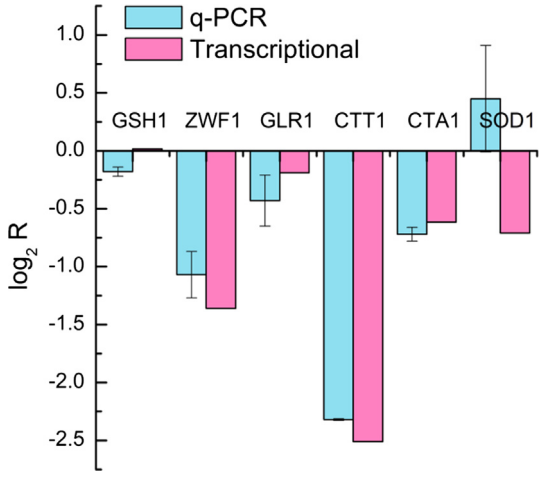


**Fig. 6.** Effect of redox potential regulation on the genes involved in the response to oxidative stress. R: Relative gene expression of −100 mV to No-aeration condition. γ-glutamylcysteine synthetase (*GSH1*), glucose 6-phosphate dehydrogenase (*ZWF1*), glutathione reductase (*GLR1*), catalase T and A (*CTT1* and *CTA1*, respectively), Cu/Zn-superoxide dismutase (*SOD1*). Error bars indicate standard deviation of biological triplicates.

respectively (Nishimoto et al., 2015), which decompose hydrogen peroxide to water and oxygen; SOD1 and SOD2 encoding cytoplasmic and mitochondrial superoxide dismutases, respectively, clear up superoxide, one major member of ROS (Azad et al., 2014); The *GRX2* gene encodes glutaredoxin that is oxidized by substrates and reduced non-enzymatically by glutathione (Rouhier et al., 2010); *TRX2* encodes thioredoxin which is reduced by thioredoxin reductase that specifically reduces glutaredoxin (Gómezpastor et al., 2012); *GLR1* encodes glutathione reductase that converts oxidized glutathione to reduced glutathione; *GPX1* encodes glutathione peroxidase which reduces free hydrogen peroxide to water and is involved in glutathione metabolism, which is the main pathway to overcome the ROS (Magnus et al., 2013; Ohdate et al., 2010); and *ZWF1* encodes glucose-6-phosphate dehydrogenase that catalyses the first step of the pentose phosphate pathway which reduces $NADP^+$ to NADPH (Partow et al., 2017).

The expression of these stress-responsive genes is closely related to the presence of furfural, which is clearly indicative that furfural induced the oxidative stress. The early degradation of furfural allows the cell to divert the energy and carbon flux used for stress-responsive protein synthesis to pathways that support better cell growth. The −100 mV ORP group was able to degrade furfural faster and consequently attain the greatest measured biomass with the highest ethanol titer among the groups tested.

## 4. Conclusions

ORP control by aeration was proven to be a simple strategy to improve the tolerance of *S. cerevisiae* to furfural. Higher ORP levels benefited yeast growth, glucose utilization, ethanol production and furfural degradation. However, controlling ORP at −100 mV was optimal for obtaining the highest ethanol titer, and the intracellular redox pairs NADH/$NAD^+$ and GSH/GSSG as well as their redox profiles were regulated, which consequently alleviated ROS damage caused by furfural. Transcriptional analysis conformed that the ORP control enhanced ethanol production and furfural degradation by shifting genes expression related to carbohydrate metabolism. With early furfural degradation, the expression of genes for stress response was down-regulated, which consequently saved energy and carbon flux for better proliferation. This strategy could be employed to improve furfural tolerance of yeast cells without extensive metabolic engineering for robust ethanol production.

## Conflict of interest

We declare that we do not have any commercial or associative interest that represents a conflict of interest in connection with the work submitted.

## Acknowledgments

This work was financially supported by the National Natural Science Foundation of China, China with grant numbers of 21536006 and 51561145014 as well as the Natural Science Foundation of Shanghai, China with grant number of 18ZR1420700.

## Appendix A. Supplementary material

Supplementary data to this article can be found online at https://doi.org/10.1016/j.ces.2018.11.059.

## References

Albertyn, J., Hohmann, S., Thevelein, J.M., Prior, B.A., 1994. GPD1, which encodes glycerol-3-phosphate dehydrogenase, is essential for growth under osmotic stress in *Saccharomyces cerevisiae*, and its expression is regulated by the high-osmolarity glycerol response pathway. Mol. Cell. Biol. 14, 4135–4144. https://doi.org/10.1128/MCB.14.6.4135.

Allen, S.A., Clark, W., Mccaffery, J.M., Zhen, C., Lanctot, A., Slininger, P.J., Liu, Z.L., Gorsich, W.S., 2010. Furfural induces reactive oxygen species accumulation and cellular damage in *Saccharomyces cerevisiae*. Biotech. Biofuels 3, 2–12. https://doi.org/10.1186/1754-6834-3-2.

Azad, G.K., Singh, V., Tomar, R.S., 2014. Assessment of the biological pathways targeted by isocyanate using N-succinimidyl N-methylcarbamate in budding yeast *Saccharomyces cerevisiae*. Plos One 9, e92993–e93104. https://doi.org/10.1371/journal.pone.0092993.

Bogengruber, E., Briza, P., Doppler, E., Wimmer, H., Koller, L., Fasiolo, F., Senger, B., Hegemann, J.H., Breitenbach, M., 2003. Functional analysis in yeast of the Brix protein superfamily involved in the biogenesis of ribosomes. Fems Yeast Res. 3, 35–43. https://doi.org/10.1111/j.1567-1364.2003.tb00136.x.

Bonnerot, C., Pintard, L., Lutfalla, G., 2003. Functional redundancy of Spb1p and a snR52-dependent mechanism for the 2'-O-ribose methylation of a conserved rRNA position in yeast. Mol. Cell. 12, 1309–1315. https://doi.org/10.1016/S1097-2765(03)00435-0.

Chen, H., Liu, J., Chang, X., Chen, D., Xue, Y., Liu, P., Lin, H., Han, S., 2017. A review on the pretreatment of lignocellulose for high-value chemicals. Fuel. Process. Technol. 160, 196–206. https://doi.org/10.1016/j.fuproc.2016.12.007.

Drakulic, T., Temple, M.D., Guido, R., Jarolim, S., Breitenbach, M., Attfield, P.V., Dawes, I.W., 2005. Involvement of oxidative stress response genes in redox homeostasis, the level of reactive oxygen species, and ageing in *Saccharomyces cerevisiae*. FEMS Yeast Res. 5, 1215–1228. https://doi.org/10.1016/j.femsyr.2005.06.001.

Gómezpastor, R., Péreztorrado, R., Matallana, E., 2012. Modification of the TRX2 gene dose in *Saccharomyces cerevisiae* affects hexokinase 2 gene regulation during wine yeast biomass production. Appl. Microbiol. Biotech. 94, 773–787. https://doi.org/10.1007/s00253-011-3738-9.

Graef, M.R.D., Alexeeva, S., Snoep, J.L., Mattos, M.J.T.D., 1999. The steady-state internal redox state (NADH/NAD) reflects the external redox state and is correlated with catabolic adaptation in *Escherichia coli*. J. Bacteriol. 181, 2351–2357.

Holm, A.K., Blank, L.M., Oldiges, M., Schmid, A., Solem, C., Jensen, P.R., Vemuri, G.N., 2010. Metabolic and transcriptional response to cofactor perturbations in *Escherichia coli*. J. Biol. Chem. 285, 17498–17506. https://doi.org/10.1074/jbc.M109.095570.

Jayakody, L.N., Horie, K., Hayashi, N., Kitagaki, H., 2014. Engineering redox cofactor utilization for detoxification of glycolaldehyde, a key inhibitor of bioethanol production, in yeast *Saccharomyces cerevisiae*. Appl. Microbiol. Biotechnol. 98. https://doi.org/10.1007/s00253-013-4997-4. 6523-6523.

Jung, Y.H., Kim, S., Yang, J., Seo, J.H., Kim, K.H., 2017. Intracellular metabolite profiling of *Saccharomyces cerevisiae* evolved under furfural. Microb. Biotech. 10, 395–404. https://doi.org/10.1111/1751-7915.12465.

Liu, C.G., Hao, X.M., Lin, Y.H., Bai, F.W., 2016. Redox potential driven aeration during very-high-gravity ethanol fermentation by using flocculating yeast. Sci. Rep. 6, 25763. https://doi.org/10.1038/srep25763.

Liu, C.G., Xue, C., Lin, Y.H., Bai, F.W., 2013. Redox potential control and applications in microaerobic and anaerobic fermentations. Biotech. Adv. 31, 257–265. https://doi.org/10.1016/j.biotechadv.2012.11.005.

Liu, Z.L., Slininger, P.J., Dien, B.S., Berhow, M.A., Kurtzman, C.P., Gorsich, S.W., 2004. Adaptive response of yeasts to furfural and 5-hydroxymethylfurfural and new

chemical evidence for HMF conversion to 2,5-bis-hydroxymethylfuran. J. Ind. Microbiol. Biotech. 31 (8), 345. https://doi.org/10.1007/s10295-004-0148-3.
Lynd, L.R., Liang, X., Biddy, M.J., Allee, A., Cai, H., Foust, T., Himmel, M.E., Laser, M.S., Wang, M., Wyman, C.E., 2017. Cellulosic ethanol: status and innovation. Curr. Opin. Biotech. 45, 202–211. https://doi.org/10.1016/j.copbio.2017.03.008.
Magnus, A., Valeria, M., Heidi, H., Lisbeth, O., Maurizio, B., 2013. Engineering glutathione biosynthesis of *Saccharomyces cerevisiae* increases robustness to inhibitors in pretreated lignocellulosic materials. Microb. Cell Fact. 12, 87–97. https://doi.org/10.1186/1475-2859-12-87.
Medina, V.G., Almering, M.J.H., Maris, A.J.A.V., Pronk, J.T., 2010. Elimination of glycerol production in anaerobic cultures of a *Saccharomyces cerevisiae* strain engineered to use acetic acid as an electron acceptor. Appl. Environ. Microbiol. 76, 190–195. https://doi.org/10.1128/AEM.01772-09.
Ming, W.L., Dale, B.E., 2009. Cellulosic ethanol production from AFEX-treated corn stover using *Saccharomyces cerevisiae* 424A(LNH-ST). P. Natl. Acad. Sci. USA 106, 1368–1373. https://doi.org/10.1073/pnas.0812364106.
Navarro-Aviño, J.P., Prasad, R., Miralles, V.J., Benito, R.M., Serrano, R., 1999. A proposal for nomenclature of aldehyde dehydrogenases in *Saccharomyces cerevisiae* and characterization of the stress-inducible ALD2 and ALD3 genes. Yeast. 15, 829–842. https://doi.org/10.1002/(SICI)1097-0061(199907)15:10A<829: AID-YEA423>3.0.CO;2-9.
Nishimoto, T., Furuta, M., Kataoka, M., Kishida, M., 2015. Important role of catalase in the cellular response of the budding yeast *Saccharomyces cerevisiae* exposed to ionizing radiation. Curr. Microbiol. 70, 404–407. https://doi.org/10.1007/s00284-014-0733-2.
Ohdate, T., Kita, K., Inoue, Y., 2010. Kinetics and redox regulation of Gpx1, an atypical 2-Cys peroxiredoxin, in *Saccharomyces cerevisiae*. FEMS Yeast Res. 10, 787–790. https://doi.org/10.1111/j.1567-1364.2010.00651.x.
Partow, S., Hyland, P.B., Mahadevan, R., 2017. Synthetic rescue couples NADPH generation to metabolite overproduction in *Saccharomyces cerevisiae*. Metab. Eng. 43, 64–70. https://doi.org/10.1016/j.ymben.2017.08.004.
Prieto, C., Risueño, A., Fontanillo, C., Rivas, J.D.L., 2008. Human gene coexpression landscape: confident network derived from tissue transcriptomic profiles. Plos One 3, e3911–e3917. https://doi.org/10.1371/journal.pone.0003911.
Qiu, Z., Jiang, R., 2017. Improving *Saccharomyces cerevisiae* ethanol production and tolerance via RNA polymerase II subunit Rpb7. Biotech. Biofuels 10, 125–131. https://doi.org/10.1186/s13068-017-0806-0.
Rouhier, N., Couturier, J., Johnson, M.K., Jacquot, J.P., 2010. Glutaredoxins: roles in iron homeostasis. Trends Biochem. Sci. 35, 43–52. https://doi.org/10.1016/j.tibs.2009.08.005.
Schrader, Sabine, Dehmlow, Eckehard Volker, 2000. Hydrogen peroxide and air as inexpensive oxidants in phase-transfer catalysis. A review. Org Prep. Proced. 32, 123–152. https://doi.org/10.1080/00304940009356279.
Sato, K., Aoki, M., Noyori, R., 1998. ChemInform abstract: a "Green" route to adipic acid: direct oxidation of cyclohexenes with 30 percent hydrogen peroxide. Science 281, 1646–1647. https://doi.org/10.1126/science.281.5383.1646.
Schafer, F.Q., Buettner, G.R., 2001. Redox environment of the cell as viewed through the redox state of the glutathione disulfide/glutathione couple. Free Radical Biol. Med. 30, 1191–1212. https://doi.org/10.1016/S0891-5849(01)00480-4.
Soltanieh, S., Lapensée, M., Dragon, F., 2014. Nucleolar proteins Bfr2 and Enp2 interact with DEAD-box RNA helicase Dbp4 in two different complexes. Nucleic Acids Res. 42, 3194–3206. https://doi.org/10.1093/nar/gkt1293.
Taherzadeh, M.J., Gustafsson, L., Niklasson, C., Lidén, G., 2000. Inhibition effects of furfural on aerobic batch cultivation of *Saccharomyces cerevisiae* growing on ethanol and/or acetic acid. J. Biosci. Bioeng. 90, 374–380. https://doi.org/10.1016/S1389-1723(01)80004-9.
Wallace-Salinas, V., Gorwa-Grauslund, M.F., 2013. Adaptive evolution of an industrial strain of *Saccharomyces cerevisiae* for combined tolerance to inhibitors and temperature. Biotech. Biofuel. 6, 1–9. https://doi.org/10.1186/1754-6834-6-151.
Wang, G.S., Lee, J.W., Zhu, J.Y., Jeffries, T.W., 2011. Dilute acid pretreatment of corncob for efficient sugar production. Appl. Biochem. Biotech. 163, 658–668. https://doi.org/10.1007/s12010-010-9071-4.
Wang, S., He, Z., Yuan, Q., 2017. Xylose enhances furfural tolerance in *Candida tropicalis* by improving NADH recycle. Chem. Eng. Sci. 158, 37–40. https://doi.org/10.1016/j.ces.2016.09.026.
Wang, X., Liang, Z., Jin, H., Bao, X., Yu, S., 2016. Identification and functional evaluation of the reductases and dehydrogenases from *Saccharomyces cerevisiae* involved in vanillin resistance. BMC Biotech. 16, 31. https://doi.org/10.1186/s12896-016-0264-y.
Zhang, Z., Li, S., Liu, L., Wang, L., Xiao, X., Sun, Z., Wang, X., Wang, C., Wang, M., Li, L., 2016. Environmental exposure to BDE47 is associated with increased diabetes prevalence: evidence from community-based case-control studies and an animal experiment. Sci. Rep. 6, 27854–27861. https://doi.org/10.1038/srep27854.
Zhang, Z., Sun, Z.Z., Xiao, X., Zhou, S., Wang, X.C., Gu, J., Qiu, L.L., Zhang, X.H., Xu, Q., Zhen, B., 2013. Mechanism of BDE209-induced impaired glucose homeostasis based on gene microarray analysis of adult rat liver. Arch. Toxicol. 87, 1557–1567. https://doi.org/10.1007/s00204-013-1059-8.
Zheng, Q., Wang, X.J., 2008. GOEAST: a web-based software toolkit for Gene Ontology enrichment analysis. Nucleic Acids Res. 36, 358–363. https://doi.org/10.1093/nar/gkn276.